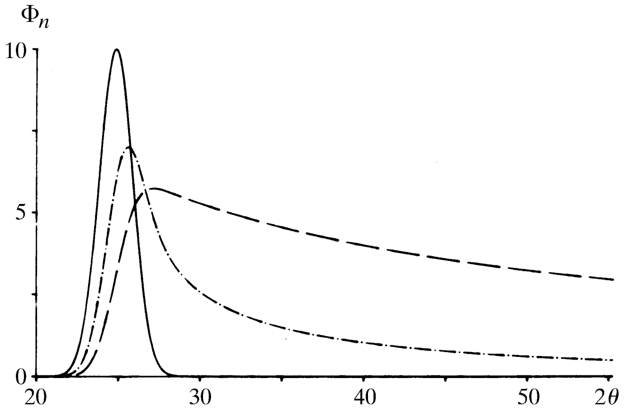

Fig. 4.2.5.2. Line profiles in powder diffraction for sharp and diffuse reflections; peaks (full line), continuous streaks (dot–dash lines) and continuous planes (broken lines). For explanation see text.

(*a*) *Isotropic diffuse peak around* τ

$$\Phi_0 = [2\pi(M^2+D^2)]^{-1/2}\cdot 1/\tau^2 \times \exp\{-(\mathbf{H}_0-\tau)^2/2(M^2+D^2)\}. \quad (4.2.5.13)$$

The moduli $|\mathbf{H}_0|$ and $|\tau|$ enter the exponential, *i.e.* the variation of $\mathrm{d}\sigma/\mathrm{d}\Omega$ along $|\mathbf{H}_0|$ is essential. For broad diffuse peaks $(M \ll D)$ the angular dependence is due to $1/\tau^2$, *i.e.* proportional to $1/\sin^2\theta$. This result is valid for diffuse peaks of any shape.

(*b*) *Diffuse streak*

$$\Phi_1 = 2\pi(M^2+D^2)^{-1/2}\int(\tau^2+q^2)^{-1/2} \times \exp\{-\mathbf{H}_0-\sqrt{\tau^2+q^2}/2(M^2+D^2)\}\,\mathrm{d}q. \quad (4.2.5.14)$$

The integral has to be evaluated numerically. If (M^2+D^2) is not too large, the term $1/k_0^2 = 1/(\tau^2+q^2)$ varies only slowly compared to the exponential term and may be kept outside the integral, setting it approximately to $1/H_0^2$.

(*c*) *Diffuse plane (with* $r^2 = q_x^2+q_y^2$*)*

$$\Phi_2 = (M^2+D^2)^{-1/2}\int r^2/(\tau^2+r^2) \times \exp\{-\mathbf{H}_0-\sqrt{\tau^2+r^2}/2(M^2+D^2)\}\,\mathrm{d}r. \quad (4.2.5.15)$$

With the same approximation as in (*b*) the expression may be simplified to

$$\Phi_2 = \pi/\mathbf{H}_0[1-\mathrm{erf}\{(\tau-\mathbf{H}_0)/\sqrt{2(M^2+D^2)}\} + 1/\mathbf{H}_0^2\sqrt{2\pi(M^2+D^2)} \times \exp\{-(\mathbf{H}_0-\tau)^2/2(M^2+D^2)\}]. \quad (4.2.5.16)$$

(*d*) *Slowly varying diffuse scattering in three dimensions*
$\Phi_3 = \text{constant}$.

Consequently, the intensity is directly proportional to the cross section. The characteristic functions Φ_0, Φ_1 and Φ_2 are shown in Fig. 4.2.5.2 for equal values of τ and D. Note the relative peak shifts and the high-angle tail.

Techniques for the measurement of diffuse scattering using a *white* spectrum are common in neutron diffraction. Owing to the relatively low velocity of thermal or cold neutrons, time-of-flight (TOF) methods in combination with time-resolving detector systems, placed at a fixed angle 2θ, allow for a simultaneous recording along a radial direction through the origin of reciprocal space (see, *e.g.*, Turberfield, 1970; Bauer *et al.*, 1975). The scan range is limited by the Ewald spheres corresponding to $\lambda_{\max}$ and $\lambda_{\min}$, respectively. With several such detector systems placed at different angles, several scans may be carried out simultaneously during one neutron pulse. There is a renaissance of these methods in combination with high-flux pulsed neutron sources.

An analogue of neutron TOF diffractometry in the X-ray case is a combination of a white source of X-rays and an energy-dispersive detector. This technique, which has been known in principle for a long time, suffered from relatively weak white sources. With the development of high-power X-ray generators or the powerful synchrotron source this method has become highly interesting in recent times. Its use in diffuse-scattering work (in particular, resolution effects) is discussed by Harada *et al.* (1984).

Valuable developments with a view to diffuse-scattering work are multidetectors (see, *e.g.*, Haubold, 1975) and position-sensitive detectors for X-rays (Arndt, 1986*a*) and neutrons (Convert & Forsyth, 1983). A linear position-sensitive detector allows one to record a large amount of data at the same time, which is very favourable in powder work and also in diffuse scattering with single crystals. By combining a linear position-sensitive detector and the TOF method a whole area in reciprocal space is accessible simultaneously (Niimura *et al.*, 1982; Niimura, 1986). At present, area detectors are mainly used in combination with low-angle scattering techniques, but are also of growing interest for diffuse-scattering work (Arndt, 1986*b*).

references